Single-Phase Mixed Molybdenum-Niobium Carbides: Synthesis, Characterization and Multifunctional Catalytic Behavior in Toluene Conversion

*Ali Mehdad, Rolf E. Jentoft,[§] and Friederike C. Jentoft[§,]**

School of Chemical, Biological & Materials Engineering
University of Oklahoma, Norman, OK 73019, USA

[§]present address: Department of Chemical Engineering, University of Massachusetts, 159 Goessmann Laboratory, 686 North Pleasant Street, Amherst, MA 01003-9303,
* Author to whom correspondence should be addressed: Email fcjentoft@umass.edu

Abstract

Single phase mixed molybdenum-niobium carbides were synthesized to establish structure–activity relationships. Precursors for carburization were obtained by hydrothermal synthesis or, to achieve high molybdenum content (metal fraction x_{Mo}=0.86), by flash-freezing of salt solutions and subsequent freeze-drying. Thermogravimetric and evolved gas analysis during carburization showed that bimetallic precursors were more easily reduced than monometallic ones; and as the niobium content increased, the removal of oxygen shifted to higher temperatures and from H_2O to CO formation (from H_2 or CH_4, respectively), and the final carburization temperature rose from 650 to 950 °C. Carbides crystallized in cubic NbC/MoC(*cF*8) structure for $x_{Nb} \geq 0.38$ and hexagonal Mo_2C(*hP*3) structure for $x_{Nb} \leq 0.14$. After passivation, mixed metal carbides could be reduced at lower temperatures than Mo_2C. With increasing molybdenum content of the carbides, CO uptake per gram increased, and turnover frequencies for hydrogenation of toluene to methylcyclohexane increased from 0 to 3.1 s^{-1} (at a temperature of 250 °C, 21 bar pressure, and H_2/toluene = 36). At 400 °C, mixed carbides with $x_{Nb} \geq 0.38$ were more selective toward acid-catalyzed products and less selective toward hydrogenolysis products than carbides with lower niobium content.

Keywords: Transition Metal Carbides, Solid Solutions, Thermal Analysis, X-ray Diffraction, Ring Contraction, Ethylcyclopentane, Methylcyclohexane, Dealkylation

1 Introduction

Transition metal carbides exhibit catalytic behavior reminiscent of that of noble metals while being less expensive and more tolerant toward some poisons [1-4]. Carbides of molybdenum or tungsten have shown promise as catalysts for, among other reactions, hydrocarbon transformations [1,2], hydrotreating [5], hydrodeoxygenation of biomass-derived molecules [6,7], and electrode reactions in fuel cells [8]. To optimize the catalytic behavior and to expand the applications of carbides, it is desirable to be able to tune their properties. A strategy offering potential to control the properties of a particular transition metal carbide is the partial substitution of anions or cations in the carbide bulk or near the surface.

With respect to anion substitution, oxide is the most widely tested species, followed by nitride [9]. The effect of introducing oxygen to carbides has been investigated by several groups emphasizing different aspects, with experimental work including both surface modification [10-12] and the synthesis of bulk oxycarbides [13-15]. DFT calculations [16] show that oxygen adsorbs strongly on the surface of molybdenum carbide, consistent with the pyrophoric nature of Mo_2C with a clean surface. Tungsten carbide is also oxophilic [10,17]. The presence of oxygen on the surface generally reduces the surface affinity for carbon [16] and the catalytic behavior moves away from that of a typical noble metal [18]; for example, hydrogenolysis is suppressed [10,12]. In addition, the presence of oxygen may result in acid sites, thus creating a bi-functional catalyst [11,12]. One problem with this type of catalyst is that oxygen may be removed in H_2-containing atmosphere; this reduction occurs at 300 °C for Mo_2C and 400 °C for W_2C at atmospheric H_2 pressure [17]. The stability of the catalyst under reaction conditions for many of the transformations listed above is thus not necessarily a given.

Regarding cation substitution, a variety of attempts have been made to synthesize mixed metal carbides, and their catalytic behavior typically differs from that of the two respective monometallic carbides. Examples include mixed molybdenum-tungsten carbides, which Leclercq et al. [19] found to be enriched in molybdenum on the surface and to exhibit complex behavior in cyclohexane dehydrogenation, and butane isomerization and hydrogenolysis. Oyama and co-workers reported bulk mixed molybdenum–niobium carbides to have promising performance in the hydrodesulfurization (HDS) of dibenzothiophene [20] and alumina-supported molybdenum-niobium carbides to be better catalysts for HDS than Mo_2C/Al_2O_3 and to have higher HDS and

hydrodenitogenation (HDN) activities per active site compared to commercial sulfided Ni-Mo/Al_2O_3 [21]. Green and co-workers published a series of papers [22-27] on combining tungsten or molybdenum with cobalt or nickel to give bimetallic carbides, which were mainly tested for hydrotreating but also for methane partial oxidation.

Anion and cation substitution have also been combined. Principally, synergy appears possible if, for example, a second cation of higher oxophilicity assists in retaining oxygen on the surface at high temperatures. For example, vanadium reportedly delays the reduction process during carburization of molybdenum oxide to molybdenum carbide [28]. In another report, mixed molybdenum-niobium oxycarbides showed better HDS and HDN activity compared to the monometallic compounds [29].

Synthesis of bimetallic carbides is generally a challenge. Metallurgical methods are excluded because they do not lead to high-surface-area materials. Like monometallic carbides, bimetallic carbides have also been made by temperature-programmed carburization of suitable precursor materials. Precursors have been generated in various ways, by physically mixing the individual oxides [20], by fusing the oxides in a high-temperature reaction [29,30], or by combining nitrates and oxides [23]. Attempts have been reported to obtain oxide solid solutions via calcination of precipitates [28,31] or reduction of calcined co-precipitates under mild conditions [32]. A variation of the oxide path is to first form a nitride and then a carbide. Sulfides have been used as precursors in carburizations to produce mixed molybdenum–tungsten carbides [33]. In sum, there are few reports of phase-pure materials over a wide range of compositions [32].

The goal of this paper is to develop methods for the synthesis of single phase mixed metal carbides over a range compositions such that structure–activity relationships can be established. To have an observable effect, molybdenum is combined with the more oxophilic niobium. The pure carbides obtained by temperature-programmed reduction, Mo_2C(*hP*3) and NbC(*cF*8), have different stoichiometries and structures. In hydrotreating and butane conversion, Mo_2C is more active than NbC [34,35]. A secondary effect of cation substitution is the change in affinity to oxygen, which can make oxycarbides stable under a wider range of conditions; and niobium reportedly should be prone to retain oxygen [29] and introduce acid sites. Hydrothermal synthesis [36] or flash-freezing followed by freeze-drying [37,38] are used to produce precursors with intimately mixed metals, which are subsequently carburized. Toluene is employed as the reactant,

and the selectivity toward ring hydrogenation and hydrogenolysis is used to assess the metallic properties, while the selectivity toward ring contraction and isomerization is used to assess the acidic properties.

2 Experimental section

2.1 Carbide synthesis

2.1.1 Synthesis of precursors

Hydrothermal synthesis was one of two methods to obtain molybdenum-niobium precursors with intimately mixed metal ions. The procedure described by Murayama et al. [36] was followed with some modifications. Ammonium heptamolybdate (AHM) (ACS reagent, 81-83% MoO_3, Sigma Aldrich) was dissolved in 0.5 M oxalic acid (anhydrous, purity>99%, Sigma-Aldrich), and ammonium niobate (V) oxalate hydrate (ANOH) (99.99%, Aldrich) was dissolved in water. The amount of salt in each solution was adjusted to give a total salt load of 4 g in 100 ml of the mixed solution while varying the metal ratios. Salt solutions were combined and mixed by stirring for 15 min. The following niobium mole fractions x_{Nb} (considering only the metals, i.e. $x_{Nb} = n_{Nb}/(n_{Mo}+n_{Nb})$) were prepared: 1.0 (ANOH-HT), 0.5, 0.33, 0.2, 0.14, 0.05 and 0 (AHM-HT). The clear solution was transferred to the 250 ml Teflon liner of a stainless-steel autoclave. The autoclave was heated to a temperature of 175 °C for 3 days under static conditions. After 3 days, the suspension was centrifuged to separate any solids from the mother liquor. The solid was washed three times with water, and then dried over night at 80 °C in an oven.

To obtain stoichiometries that were not accessible by hydrothermal synthesis, mixed metal precursors were produced by flash-freezing and freeze-drying. Appropriate amounts of ammonium heptamolybdate and ammonium niobate oxalate hydrate were dissolved separately in water and mixed together to obtain various metal ratios with a final total metal concentration of 0.1 M. The solution was added dropwise to liquid N_2. Globules of the frozen solution were recovered, and freeze-dried at a pressure of 110 µtorr in an ATR FD3.0 freeze drier.

2.1.2 Equipment for thermal treatments and gases

A Netzsch STA 449 F1 thermogravimetric analyzer (TGA) was connected to a mass spectrometer (QMS 403 C Aëolos) via a stainless-steel capillary. Temperature-programmed reaction runs with empty crucibles were used to correct for sample holder buoyancy and gas

viscosity artifacts. MS signals were generally normalized to initial sample mass. Methane (UHP, Airgas) was used as received; other gases were further purified prior to use. Air (zero grade, Airgas) and H_2 (ultra-high purity, Airgas) were passed through a moisture trap (Agilent, MT400-2), and argon (ultra-high purity, Airgas) was passed through dual moisture and oxygen trap (Z-Pure Dual Purifier). All flow rates are given at STP, all percentages by volume.

2.1.3 Calcination of freeze-dried samples

Freeze-dried samples (AHM-FD, ANOH-FD and a mixed metal sample with $x_{Nb} = 0.13$) were calcined in the TG apparatus in 80% air in argon at a total flow rate of 50 ml/min. The temperature was increased from 40 to 600 °C with a temperature ramp of 5 °C/min, and was held at the final temperature for 30 min.

2.1.4 Carburization and passivation

Precursors were carburized in the TG-MS apparatus, and mass-charge ratios of 2 to 78 were scanned during the treatments. The carburization gas was obtained by mixing 20 ml/min of methane, 70 ml/min of H_2 and 10 ml/min of argon. The synthesis of all metal carbides was carried out at atmospheric pressure by heating from 40 to 450 °C at 5 °C/min and from 450 °C to the final temperature at 2 °C/min. Samples were held at the final temperature until no weight change was observed by TG and formation of CO was terminated. All metal carbides were cooled down to room temperature under argon flow. Before exposure of the carbides to the ambient, they were passivated isothermally at 40 °C with air diluted in argon. The concentration of O_2 was increased from 0.1% (10 h) to 1% (9 h) and 16% (2 h) in argon [17], with the total flow rate between 60 and 402 ml/min.

2.2 Characterization of carbides

The bulk structure of the samples was characterized by powder X-ray diffraction (XRD) using a Bruker D8 instrument operating with Cu Kα radiation. The samples were measured in reflection geometry after mixing with nickel metal powder (Matheson Coleman & Bell, 200 mesh), which served as a reference. Diffractograms were collected by scanning in steps of 0.05 in 2θ over the angular range of 20-90°. The lattice parameters of each product were obtained by fitting the diffractograms using Powdercell software. The carbon content of the samples was measured by combustion analysis in a CE-440 Elemental Analyzer. The molybdenum and niobium concentrations were determined using energy-dispersive X-ray spectroscopy (EDS) on a JEOL

JSM-840A scanning electron microscope at an operating voltage of 15 kV and a Kevex X-ray analyzer and IXRF software with digital imaging capability. Surface areas of passivated materials were determined by the BET method using a Micromeritics ASAP 2010 and N_2 at -196 °C. Pore size distributions were determined from N_2 desorption isotherms by applying the BJH method. Before measuring the surface area, the samples were degassed at 350 °C for 4 h. The number of metal sites was measured by CO chemisorption using a Micromeritics ASAP 2020. Prior to CO chemisorption, samples were reduced in H_2 at 350 °C for 1 h and degassed for 1 h at the same temperature, then they were cooled to 35 °C and a first CO adsorption isotherm was recorded. Subsequently, weakly adsorbed CO was removed by evacuation, and a second CO adsorption isotherm was acquired. The difference between the first and the second isotherm was plotted and extrapolated to zero pressure to calculate the amount of CO chemisorbed.

2.3 Temperature-programmed reduction (TPR)

The TPR experiments were carried out in the TG-MS apparatus described in Section 2.1.2 on about 11 mg of passivated sample immediately following passivation. The total flow rate was 100 ml/min of a mixture of 80% H_2 in argon. The temperature was set to 40 °C for 10 minutes and then increased from 40 to 700 °C with a temperature ramp of 10 °C/min. Gas phase products were monitored by online MS, scanning m/z between 2 and 78.

2.4 Catalytic tests: vapor phase toluene conversion

The carbide samples were tested at temperatures of 250 °C and 400 °C in the vapor phase conversion of toluene at elevated H_2 pressure. The flow reactor was a 0.18 inch inner diameter stainless steel tube with Swagelok® connections equipped with an Eldex liquid feed pump. The reactor was loaded with varying amounts of passivated carbides that were mixed with 200 to 300 mg SiC (Aldrich, 200-450 mesh) to avoid channeling and local heating. The reactor was placed into a 2 ft long electrical furnace, and the temperature was controlled using a thermocouple inside the reactor at the bottom of the catalyst bed. All samples were reduced at atmospheric pressure in a H_2 flow of 150 ml/min at a temperature of 300 °C for 1 h before the catalytic reaction. After reduction, the reactor was cooled to 250 °C, and the back-pressure valve was set to achieve an absolute pressure of 21 bar. Then, the feed of 0.01 ml/min of liquid toluene (99.5%, Mallinckrodt Chemicals) and 75 ml/min STP H_2 (Ultra high purity, Airgas) was introduced to the reactor and the effluent stream was analyzed every 30 min. After 2.5 h of operation at 250 °C, the reactor was heated to 400 °C and was held at this temperature for 24 h, during which time the effluent stream

was sampled. Products were analyzed using an online HP 5890 GC with a flame ionization detector, equipped with a 30 m, 0.32 mm GASPRO column. Transfer lines to the GC were heated to ensure that no condensation occurred. The GC temperature program was, 5 min isothermal at 60 °C, then a temperature ramp of 10 °C/min to the final temperature of 240 °C, which was held for 4 min. Equations for the calculation of conversion, selectivity, rate, and turnover frequency are given in the supporting information. Conversion corresponds to the disappearance of toluene, and selectivity calculations account for the number of carbon atoms in each product.

3 Results

3.1 Synthesis of metal carbides

3.1.1 Precursor preparation

Precursors for carburization were prepared by two methods: hydrothermal synthesis (HT) and freeze-drying (FD). The hydrothermal synthesis method was based on the procedure reported by Murayama et al. [36], who prepared precursors for mixed metal oxides, including mixed molybdenum-niobium oxides. In this work, their method was modified by using a soluble niobium salt rather than niobium oxide and by adding acid. The molybdenum precursor was dissolved in oxalic acid to prevent immediate precipitation. The yields obtained by this method were generally low, with the weight of the recovered solid only accounting for about 20 to 30% of the charged weight of solid. In addition, the composition of the eventually obtained carbides (shown in Table 1) demonstrates that niobium was preferentially incorporated in the hydrothermally synthesized precursors over most of the compositional range. The addition of oxalic acid resulted in precursors that could be carburized at a lower final temperature than those prepared in the absence of acid; moreover, the final carbides were characterized by smaller particles than those from precursors prepared without oxalic acid. All presented hydrothermally synthesized materials were prepared with acid addition. The hydrothermally prepared precursors were X-ray amorphous. The method of flash-freezing followed by freeze-drying obviously implies quantitative use of the salts and a precursor that has the intended metal composition. The precursors prepared by the HT method were directly carburized, whereas the precursors prepared by the FD method, which incorporate all ions from the salts, were first calcined and then carburized. The intended and actual compositions of the final carbides are reported in Table 1.

3.1.2 Carburization of hydrothermally synthesized precursors

Precursors with an intended niobium mole fraction x_{Nb} of 0.0, 0.05, 0.14, 0.33, 0.50 and 1.0 gave mixed metal carbides that contained more niobium than intended. The measured metal composition (Table 1) will be used in the following to discuss the precursor behavior.

Precursors with x_{Nb} of 0.0, 0.13, 0.38, 0.51, 0.70 and 1.0 lost 35.5, 31.4, 28.8, 27.3, 28.0 and 30.0 % of their initial weight, respectively, when carburized without prior calcination (Figure 1). For comparison, the conversion of MoO_3 to Mo_2C is associated with a weight loss of 29.2 %, and conversion of Nb_2O_5 to NbC is associated with a weight loss of 21.1 %. The fact that the observed weight losses exceed those of the stoichiometric oxides implies that the hydrothermally synthesized precursors contain additional material such as water, hydroxide or other ions from the salts. The TG traces reflect the decomposition of such species, as they exhibit more than the two steps typical of reduction to an oxide of lower metal oxidation state and carbide formation [39,40]. Multiple water formation events (Figure 1b), particularly at low temperature are probably dehydration and dehydroxylation rather than reduction steps. In addition, AHM-HT and ANOH-HT showed evolution of m/z=28 at low temperatures, which coincided with the evolution of m/z=44 for ANOH-HT, thus indicating CO_2 from oxalate. For AHM-HT, no m/z=44 was observed but instead the formation of water, consistent with one of the known decomposition pathways of oxalic acid [41].

Since hydrothermally synthesized precursors did not contain much more mass per metal than oxides and the responsible species were readily decomposed before carbide formation, such precursors were generally carburized without calcination to avoid segregation into individual oxides and loss of surface area or loss of molybdenum.

At a temperature of about 350 °C, all samples that contained molybdenum lost weight with concomitant water evolution. The formation of CO, which indicates the activation of methane and further removal of oxygen, occurred over a wide range of temperature. For AHM-HT, the maximum of CO evolution was 650 °C. The onset of CO formation for some of the mixed metal precursors occurred at temperatures even lower than that seen for AHM-HT. For samples rich in molybdenum, formation of CO was accompanied by the formation of water, whereas for samples rich in niobium, CO formation occurred without evolution of water (Figure 1b and c).

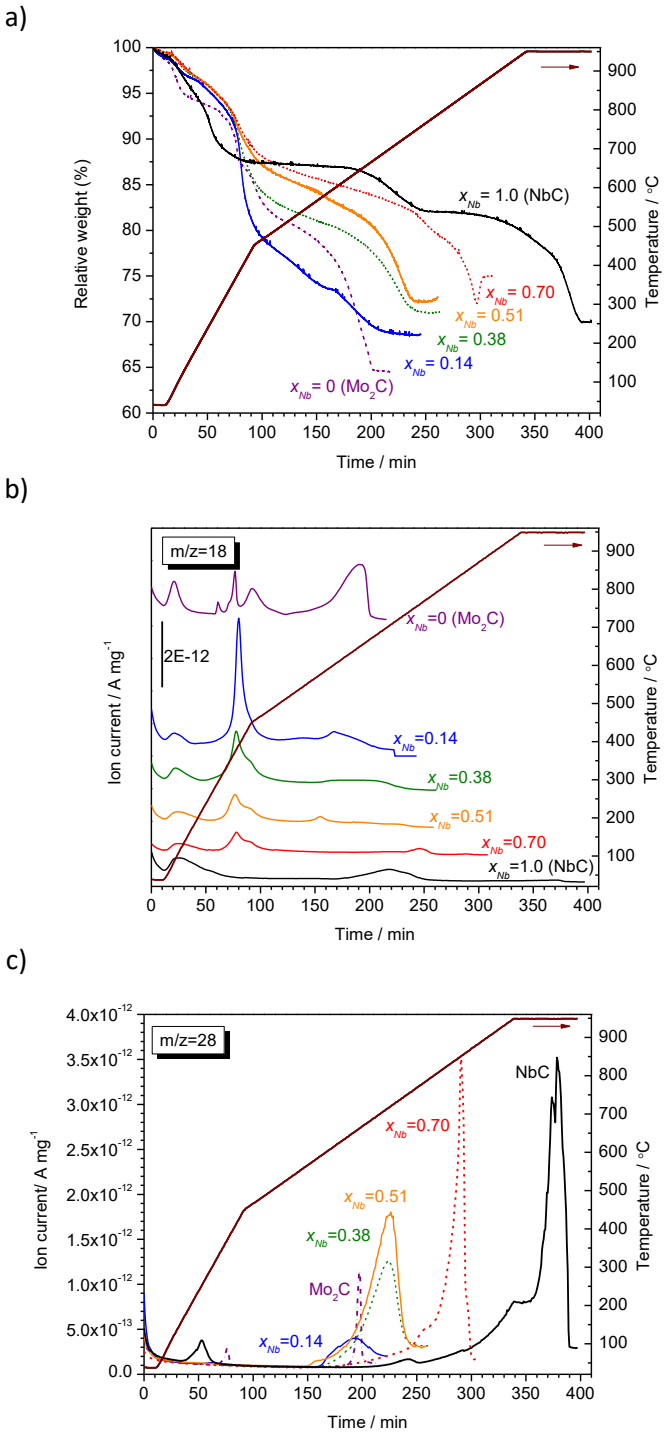

Figure 1: Direct carburization of hydrothermally prepared precursors monitored by thermogravimetry and mass spectrometry. Gas phase mixture 20% CH_4/70% H_2/10% Ar. a) Weight change, b) water formation (m/z=18) and c) CO formation (m/z=28).

240

241 There is typically an optimum final temperature, as high temperatures may promote carbon
242 deposition and sintering. The material with x_{Nb} = 0.70 was the only one that passed through a
243 minimum in weight (at 72%) and then quickly gained 3.1%. This gain was assumed to result from
244 carbon deposition on the surface and, consequently, to generate samples for the catalytic test and
245 the characterization measurements, the carburization was stopped before the material started to
246 gain weight; the chosen end point was when the weight was stable and no more CO evolved.

247 On the basis of these criteria, carburization of AHM-HT to Mo_2C required the lowest final
248 carburization temperature (680 °C), carburization of ANOH-HT to form NbC required the highest
249 temperature (950 °C), and carburization of the mixed metal precursors required temperatures of
250 650, 720, 720, 850 °C for niobium fractions x_{Nb} of 0.13, 0.38, 0.51, and 0.70.

251 *3.1.3 Calcination and carburization of freeze-dried precursors*

252 Freeze-dried precursors AHM-FD, ANOH-FD and a mixed precursor with intended niobium
253 fraction x_{Nb} of 0.13 were calcined in the TG-MS apparatus at final temperatures of 500 °C (AHM-
254 FD) and 600 °C (mixed precursor and ANOH-FD). The final temperature was held until the weight
255 was stable and no more gas phase products were observed with the online MS. The niobium
256 content of the mixed carbide was later found to be x_{Nb}=0.14, and accordingly, the oxide will be
257 designated as $Mo_6NbO_{20.5}$. The XRD data for the calcined samples are reported in Figure 2. The
258 patterns of the pure oxides could be matched with ICDD: 00-005-058, orthorhombic MoO_3(*oP*16),
259 and ICCD: 00-028-0317, monoclinic Nb_2O_5(*hP*7). The pattern of $Mo_6NbO_{20.5}$ is very similar to
260 that of MoO_3 and is distinguished mainly by an additional reflection at 22.30 ° 2θ.

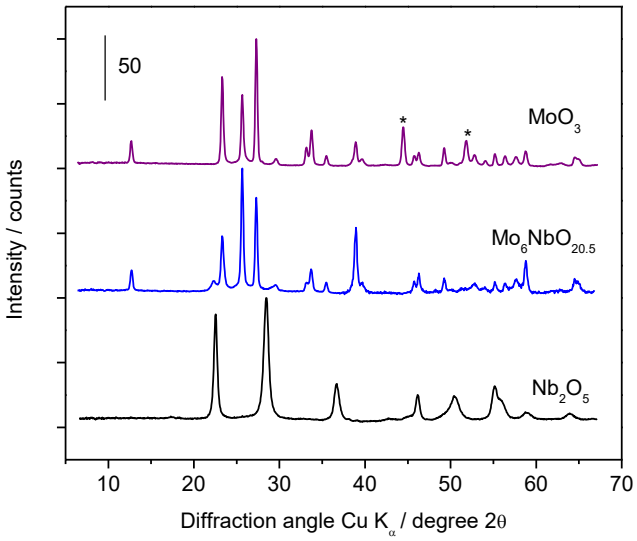

Figure 2: X-ray diffractograms of calcined precursors from flash-freezing/freeze-drying. Calcination temperatures 500 °C for MoO_3, or 600 °C for $Mo_6NbO_{20.5}$ and Nb_2O_5. Asterisks mark nickel internal standard.

The oxides obtained through calcination were carburized in the TG-MS apparatus, and the weight losses and gas phase products are reported in Figure 3. There were at least two reduction steps with water formation for all three oxides. The first water peaks were observed at 435, 570 and 720 °C, respectively, and the associated weight loss is consistent with reduction to approximately Mo_6NbO_{13}, $MoO_{1.9}$ and $NbO_{1.9}$. The second reduction step of the mixed oxide occurred at much lower temperature than those of either of the pure oxides. During the carburization of MoO_3, there was a sharp CO peak that started when the stoichiometry was about $MoO_{0.75}$ and reached its maximum at about 650 °C. For the mixed oxide, CO evolution started when the stoichiometry was about Mo_6NbO_{10}, and two maxima were observed at 600 and 660 °C. The carburization of niobium oxide was characterized by two CO peaks; a small CO peak was observed with the first peak of water at 715 °C and a large peak of CO was observed around 950 °C. Comparing relative CO and H_2O peak sizes, it is obvious that the transformation of the molybdenum-containing samples resulted in formation of more water than that of Nb_2O_5, which in contrast resulted in formation of more CO.

Because longer chain hydrocarbons are reported to lower the temperature for formation of molybdenum carbide [26], carburization of Nb_2O_5 with 10% ethane in H_2 was attempted. Phase-pure NbC could not be obtained (see the Supporting Information).

a)

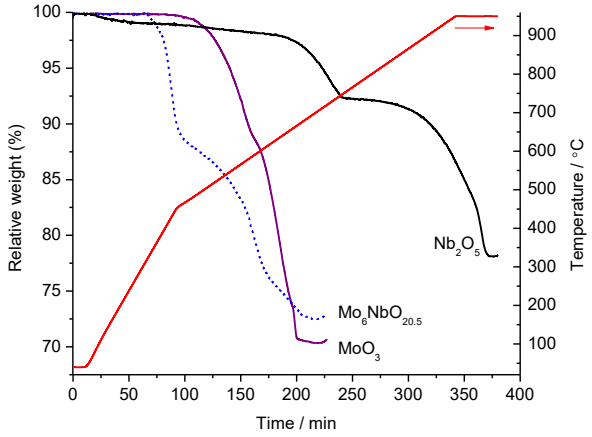

b)

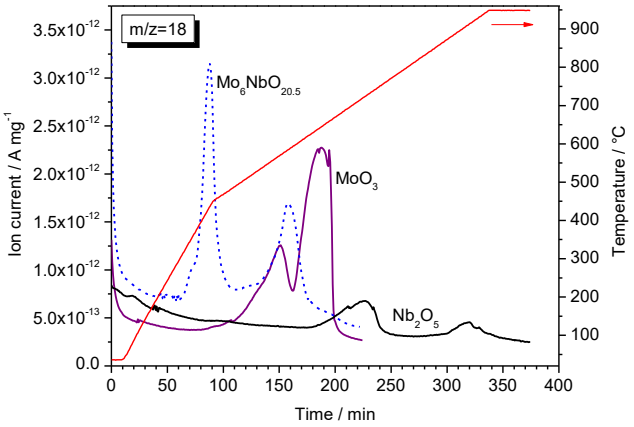

c)

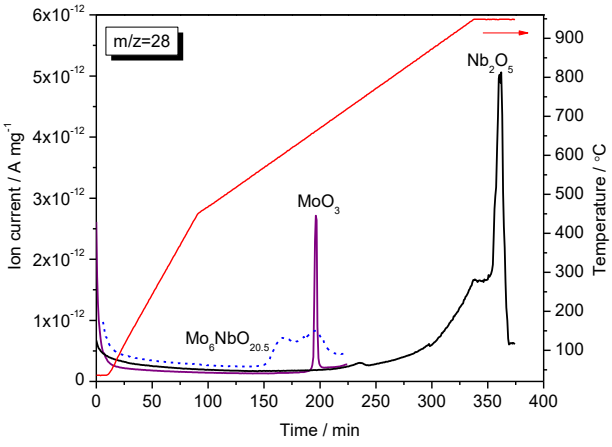

Figure 3: Carburization of calcined precursors (labels indicate starting composition) from flash-freezing/freeze-drying monitored by thermogravimetry and mass spectrometry. Gas phase mixture 20% CH_4/70% H_2/10% Ar. a) Weight change, b) water formation (m/z=18) and c) CO formation (m/z=28).

During carburization of Nb_2O_5, at 800 °C, ethylene started to evolve after the first water peak and its formation rate increased at higher temperatures. Formation of ethylene was observed with an empty crucible in the TG apparatus. However, the amount of ethylene formed was twice as large with the catalyst present.

The TG profiles and the CO evolution demonstrate that the carburization of Nb_2O_5 was completed at a very high temperature (950 °C), whereas carburization of the mixed metal oxide with $Mo_6NbO_{20.5}$ stoichiometry required the same final temperature as was needed for synthesis of Mo_2C (650 °C). Considering MoO_3, Nb_2O_5 and $Mo_6NbO_{20.5}$ as starting stoichiometries and Mo_2C, NbC and $Mo_6NbC_{3.5}$ as the product stoichiometries, the theoretical weight losses are 29.2, 21.1 and 28.7%. The observed values of 29.6, 20.8 and 27.5% are in good to very good agreement with these predictions.

3.2 Characterization of the carbides

The composition of the mixed carbides was determined by EDS. In Figure 4, the measured niobium fractions in the carbides are plotted versus the niobium fractions in the synthesis solution for the hydrothermal method. The deviation from the parity line shows that the carbides were enriched in niobium relative to the starting solutions.

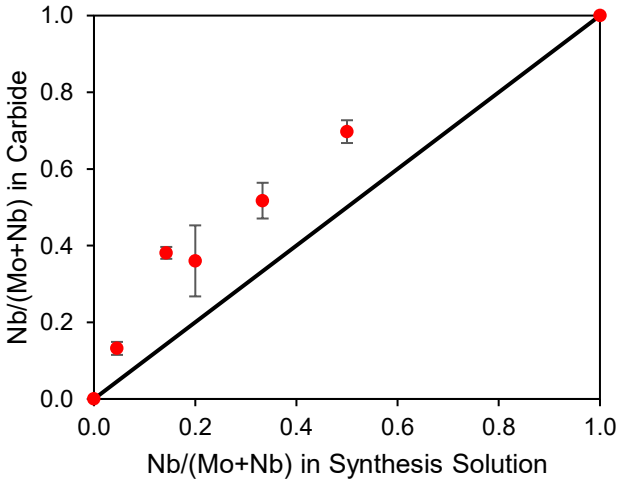

Figure 4: Niobium fraction x_{Nb} in the carbides vs. niobium fraction in the hydrothermal synthesis solution. Solid line represents parity.

The structures of the samples were analyzed by XRD, and the diffractograms are reported in Figure 5. All niobium-containing carbides with $x_{Nb} \geq 0.38$ prepared by the HT method had the cubic

296 structure of NbC(*cF*8) (ICDD: 00-038-1364), which is isostructural with cubic MoC(*cF*8) (ICDD
297 # 03-065-8092). Pure molybdenum carbide (Figure 5-11) was characterized by the hexagonal
298 structure reported for Mo_2C(*hP*3) (ICDD: 00-035-0787). A carbide with an intended x_{Nb} of 0.05
299 and an actual x_{Nb} of 0.13 prepared by carburization of a HT precursor consisted of two phases, of
300 cubic NbC/MoC and of some Mo_2C as can be seen in Figure 5-9.

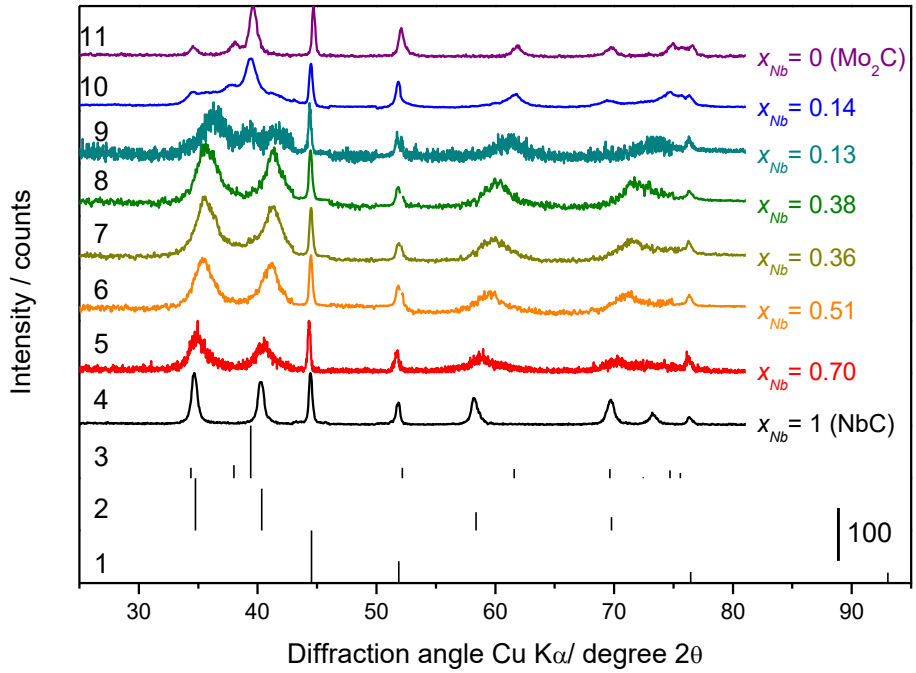

Figure 5: XRD patterns for molybdenum-niobium carbide series. Nickel used as internal standard. Patterns 1-3, references. Pattern 10, carbide from flash-frozen and freeze-dried precursor; all other patterns, carbides from hydrothermally synthesized precursors. (1) Ni (ICDD:00-004-0850) (2) NbC (ICDD:00-038-1364) (3) Mo_2C (ICDD: 00-035-0787). (4) x_{Nb} = 1.0 (5) 0.70 (6) 0.51 (7) 0.36 (8) 0.38 (9) 0.13 (10) 0.14 (11) 0.

301 To synthesize a mixed metal carbide with hexagonal Mo_2C structure, mixed metal precursors
302 containing both molybdenum and niobium were prepared by the freeze-drying method.
303 Carburization of precursors with $x_{Nb} > 0.13$ resulted in NbC structures (not shown). Direct
304 carburization of a sample with $x_{Nb} = 0.14$ led to a broad peak assigned to the (002) plane in the
305 Mo_2C structure; to overcome this problem the FD precursor was calcined and then carburized. The
306 obtained material contained hexagonal Mo_2C (Figure 5-10) and a poorly crystallized phase that
307 could be fit with cubic NbC.

The diffractograms showing the NbC/MoC structure were fit using Powdercell software, and the obtained lattice parameters of the samples are plotted versus the niobium mole fraction in Figure 6, together with reference values from the ICDD. The observed linear relationship is consistent with Vegard's Law for solid solutions. In contrast, there was no shift in the lattice parameter of the Mo_2C structure when niobium was present, suggesting that niobium does not dissolve into this structure.

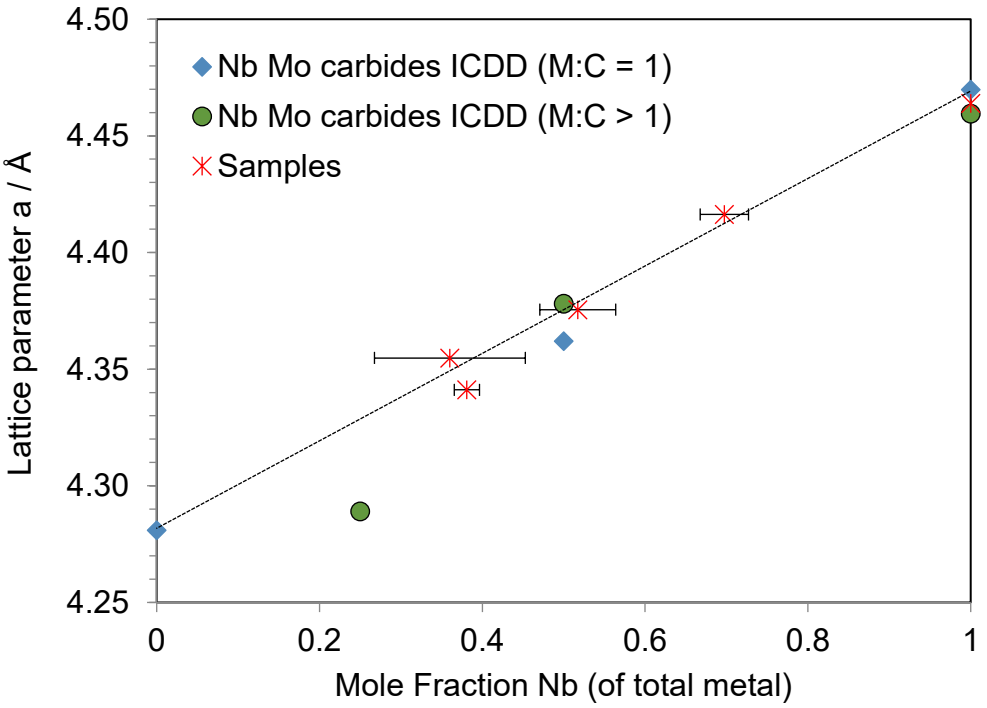

Figure 6: Lattice parameter of Mo-Nb carbides with cubic NbC/MoC structure vs. mole fraction of niobium. □ MoC (ICDD: 03-065-8092), ● (Nb/C >1, (ICDD: 03-065-8768, 03-065-7992 and 01-089-4306), ◊ (Nb/C=1, ICDD: 00-038-1364 and 3-065-8767) and Ж prepared samples. Line connects endpoints.

Compositions, weight gains after passivation, surface areas and pore size values, and CO adsorption capacities are reported in Table 1. The carbon content for Mo_2C was found to be slightly below the theoretical content and that for NbC slightly above the theoretical content. The theoretical carbon content for the mixed carbides requires an assumption of the number of carbons per metal, which could be guided by the stoichiometry of the series endpoints, or by the observed structure. Even if a stoichiometry of only one carbon atom per two molybdenum atoms and of one carbon atom per niobium atom is assumed, the mixed carbides are carbon-deficient.

Table 1: Characterization data for molybdenum-niobium carbide samples

Nb/(Mo+Nb)		T_f (°C)[b]	Carbon content (wt%)		Weight gain after passivation[d] (%)[c]	Residual oxygen[e] (%)	S_{BET} (m^2/g)[f]	BJH volume (cm^3/g)[f]	BJH pore diameter (nm)[f]	CO uptake (µmol/g)
Intended	EDX[a]		Theoretical[c]	Measured						
0.00	0.00	650	5.9	5.3±0.3	2.49	2.0	16.5	0.052	11.2	18.5
0.13[g]	0.14±0.02	650	6.7	5.5±0.3	2.85	2.3	23.7	0.079	12.0	15.0
0.14	0.38±0.02	700	8.0	6.3±0.9	5.67	4.2	58.4	0.166	11.4	13.5
0.33	0.51±0.05	700	8.8	6.8±0.9	5.80	4.4	102.2	0.134	50.0	7.7
0.50	0.70±0.03	840	9.8	8.6±0.3	1.70	1.4	57.5	0.18	100.0	2.3
1.00	1.00	950	11.4	12.0±0.2	0.00	0.0	16.7	0.088	165.2	0.0

[a]Measured on multiple particles, average and standard deviations are reported. [b]Final carburization temperature. [c]Assuming one carbon per two molybdenum atoms and one carbon per niobium atom. [d]Basis is freshly prepared carbide before exposure to air. [e]Measured at 350 °C during TPR and expressed as percentage of oxygen taken up during passivation. [f]Measured after passivation. [g]Carburization of freeze-dried precursor, all others from hydrothermally synthesized precursors.

The two carbides with Mo_2C structure gained 2.5 and 2.9 %, in weight during passivation, whereas those with NbC structure gained more than 5 % at low niobium contents (and required passivation times in 0.1% O_2 of up to 10 h). The weight gain during passivation declined at high niobium content, and in line with this trend, the surface of NbC was inert towards O_2.

The N_2 physisorption isotherms were type IV with a pore size distribution in the mesoporosity range. The surface area first increased with increasing niobium content and then decreased. The pore size increased with increasing niobium content, whereas the CO uptake per mass (and also per surface area) decreased.

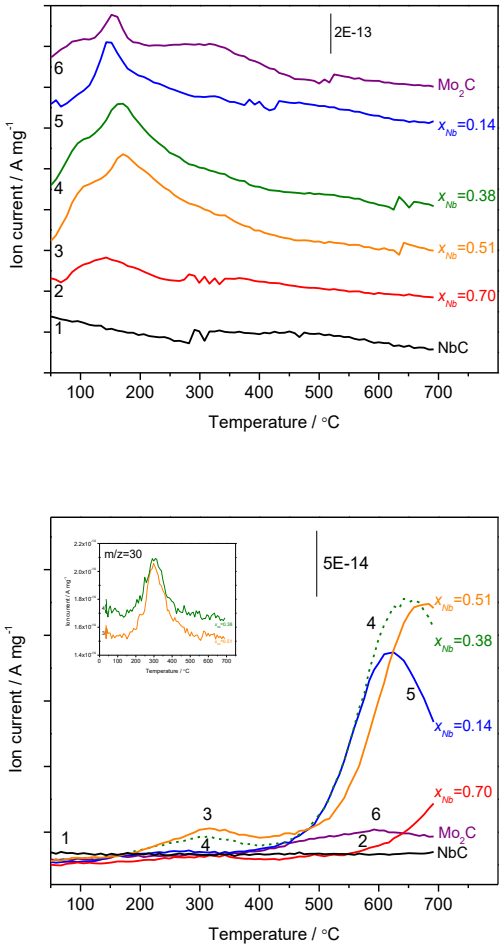

Figure 7: TPR data for Mo-Nb carbides. Formation of water (m/z=18, top), methane and ethane (m/z=15 and 30, bottom). Samples are carbides with x_{Nb} of (1) 1.0, (2) 0.70, (3) 0.51, (4) 0.38, (5) 0.14 and (6) 0. Gas phase composition: 80% H_2/Ar.

3.3 Reduction after passivation

Temperature-programmed reduction (TPR) in 80% H_2/Ar at atmospheric pressure was used to investigate the temperature range necessary to remove oxygen and carbon from the passivated materials. The TPR results are shown in Figure 7.

The main gas phase products were water (m/z=18), methane (m/z=15), and ethane (m/z=30). TPR data for NbC did not show any gas phase products, consistent with the lack of weight gain during the O_2 treatment. For all other samples, water started to form in the temperature range from 100 to 300 °C, and the intensity of the water signal scaled with the weight gained during passivation. For the niobium-rich carbides, water started to form at lower temperatures compared to the molybdenum-rich carbides, as can be seen from the peak at 100 °C for x_{Nb} of 0.38, 0.51 and 0.70 (traces 4, 3, and 2, in Figure 7). For two of the mixed metal carbides (with x_{Nb} of 0.51 and 0.38) that were prepared from HT precursors, ethane evolution was observed at about 300 °C. Methane evolved at or above 400 °C for all samples except for NbC. The maximum of the methane peaks in the mixed metal carbides shifted to higher temperatures with increasing niobium content; methane production reached its maximum at 600 °C for the carbide with $x_{Nb} = 0.14$ whereas it only began at this temperature for the carbide with $x_{Nb} = 0.70$. Pure molybdenum carbide formed a small amount of methane, whereas the mixed metal carbides rich in molybdenum formed significantly more methane.

Analysis of the weight during TPR demonstrated that at a temperature of 350 °C, 95% or more of the oxygen in the passivation layer were removed. The samples with surface areas over 50 m^2/g and a high fraction of molybdenum retained a measurable amount of oxygen in this experiment (Table 1).

On the basis of these observations, a temperature of 300 °C and a 1 h holding time in H_2 were chosen to reactivate the passivated carbides in the reactor prior to introducing toluene, with the goal of removing oxygen but not carbon.

3.4 Catalytic activity in toluene hydrogenation

Toluene hydrogenation was applied as the test reaction to determine activity, selectivity, and stability of the carbides listed in Table 1. Internal mass transfer limitations were excluded by applying the Weisz-Prater criterion (see the supplementary information). To exclude that the toluene-methylcyclohexane hydrogenation-dehydrogenation equilibrium determines the observed

product distribution [42], equilibrium compositions for the reaction between toluene, H_2 and methylcyclohexane at relevant conditions were obtained using ThermoSolver software. At a total pressure of 21 bar and a H_2 to toluene ratio of 36, applying Peng-Robinson fugacity coefficients, the equilibrium molar ratios of toluene to methylcyclohexane were found to be 1.5×10^{-5} : 1 at 250 °C and 1:1 at 400 °C. The highest toluene conversions considered were 77 % at 250 °C and 17% at 400 °C, which are sufficiently far from equilibrium limitations.

At a reaction temperature of 250 °C, the catalysts exhibited stable performance, and the product selectivity was 100% methylcyclohexane (MCH). Rates were strictly proportional to inverse space velocities up to conversions of 77 %, and turnover frequencies (TOFs) relative to the number of sites as determined by CO chemisorption were calculated using the average rate of several experiments. TOFs for ring hydrogenation of toluene at 250 °C are reported in Figure 8. The results reveal that the ring hydrogenation activity per site decreases with increasing niobium content, from a turnover frequency of slightly above 3 s^{-1} on Mo_2C to 0 s^{-1} on the inactive NbC.

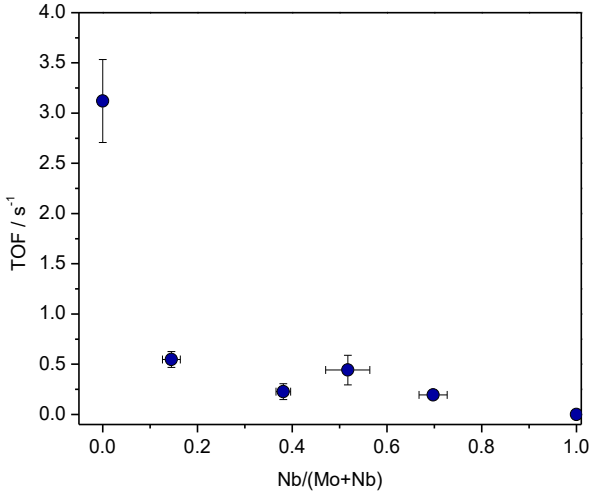

Figure 8: Turnover frequencies for ring hydrogenation of toluene vs molar fraction of niobium. Reaction conditions: temperature 250 °C, total pressure 21 bar, molar ratio of H_2 to toluene 36:1. Shown is the series of molybdenum-niobium carbides presented in Table 1.

At a reaction temperature of 400 °C, the activity of the carbide with $x_{Nb} = 0.70$ was very low (less than 2% conversion at W/F=0.25 h) and NbC was inactive. Mo_2C was the most active catalyst and by increasing the amount of niobium, the activity decreased while the stability increased. Over 24 hours on stream, all samples showed some deactivation. For Mo_2C, the loss of activity was

36%, and for carbides with niobium fractions x_{Nb} of 0.14, 0.38 and 0.51 the losses were 24, 4 and 7, respectively. The product selectivity did not change with the degree of deactivation.

Table 2: Product selectivity for mixed niobium-molybdenum catalysts at equal toluene conversion at 400 °C and 20.4 bar H_2

Nb/(Mo+Nb)	W/F (h)	Conv. (%)	Selectivity (mol%)					
			C_1-C_6	MCH	ECP	DMCP	Benz.	Xylene
0	0.01	14.9	41.9	40.9	0.0	0.0	11.6	5.6
0.14[a]	0.02	14.6	40.1	40.7	2.1	0.0	11.5	5.6
0.38	0.16	16.9	22.4	23.7	17.6	14.0	14.6	7.7
0.51	0.20	16.6	34.6	20.2	16.9	11.8	10.7	5.8

[a]Carburization of freeze-dried precursor, all others from hydrothermally synthesized precursors.

Product selectivities at comparable conversions are reported in Table 2. A weight hourly space velocity spread of one order of magnitude was necessary to achieve equal conversions. Samples rich in molybdenum showed mostly hydrogenolysis products (≈40%) and not much ethylcyclopentane (ECP) and dimethylcyclopentane (DMCP). However, adding niobium decreased the fraction of hydrogenolysis products and significantly enhanced the formation of ECP and DMCP. All samples catalyzed the formation of benzene and xylene with a benzene excess. Samples with a higher niobium content produced slightly more benzene and xylene than the molybdenum-rich carbides.

4 Discussion

4.1 Carburization of precursors

4.1.1 Formation of pure Mo_2C and NbC from uncalcined HT and calcined FD precursors

Both types of precursor were converted into carbides in several steps that can be classified into decomposition of counter ions from the salts used in the synthesis, reduction, and carbon incorporation with carbide formation. The presence of other elements in addition to metal and oxygen is unique to the uncalcined hydrothermal precursors and while seemingly making the transformation more complex, the additional steps were confined to the early stages, that is to temperatures of less than 300 °C, as can be seen by comparison of the TG traces and gas phase

products in Figure 1 with those in Figure 3. The actual reduction and carburization events depended on the metal mole fractions and were largely independent of the nature of the precursor.

The transformations of the pure oxides to carbides are described and analyzed in the literature. Reduction requires the activation of hydrogen or the hydrocarbon and may be controlled by the formation of reduced patches on the surface or by mobility of oxygen in the bulk. Carbide formation requires diffusion of carbon into the bulk. The solid state transformation of molybdenum oxide to molybdenum carbide is reported as follows: MoO_3 to MoO_2 to MoO_xC_y to Mo_2C [43]. A similar phase transformation happens during synthesis of niobium carbide: Nb_2O_5 to NbO_2 to NbO_xC_y to NbC [39]. The first reduction (Nb_2O_5 to NbO_2) [39] and also the second step (NbO_2 to NbC) [44] was inferred to be controlled by nucleation. The weight losses observed here in the first step correspond to formation of $MoO_{1.9}$ and $NbO_{1.9}$, implying predominant valences of Mo(IV) and Nb(IV) in agreement with known stable oxides of these elements and with the literature [39,43]. There is a significant difference between the two oxides with respect to the temperatures (activation energies) required for each step. The carburization temperatures of 650 °C for Mo_2C and 950 °C for NbC observed are close to literature reports of 657 °C [40] and 900 °C [39].

TG and MS data in Figure 3 show that in the first step, both oxides are reduced to an intermediate oxidation state with formation of water, implying activation of only H_2. In the second step, CO is also formed, indicating activation of methane and further reduction. The weight change and CO formation always ended simultaneously, implying that carbon incorporation and carbide formation occurred in parallel to reduction. Comparison of the intensities reveals that much more H_2O forms from molybdenum oxide than from niobium oxide, whereas the reverse applies for CO formation. These results mean that, depending on the composition of the carbide and the temperature, the surface is more likely to be covered with hydrogen or carbon, which will react with emerging oxygen to form the observed products.

During the final stage of Mo_2C formation, water is formed from both H_2 and methane, as the sharp water peak shows that coincides with CO formation (Figure 3). The weight loss during the simultaneous reduction and carburization is rapid, indicating that both oxygen removal and incorporation of carbon into the lattice are facile.

During the final stage of niobium carbide formation, only CO is released and no water (Figure 1 and Figure 3); presumably, hydrogen from methane evolves as H_2. Although the temperature is much higher, the weight loss is much slower during NbC formation than during Mo_2C formation. Notwithstanding isothermal conditions at 950 °C, there is acceleration in the weight loss, which could be explained by heightened mobility as reduction progresses and vacancies are formed. The high temperatures needed for this process and the inability of the surface to activate enough H_2 can promote carbon accumulation on the surface, which can be a problem with the synthesis of niobium carbide [45] and leads to poor catalytic activity. A variety of synthesis methods have been tested to avoid carbon contamination of NbC, with varied success. Precursors with a lower niobium oxidation state or a smaller particle size were employed, but the temperature for carbide formation could not be substantially lowered and surface contamination occurred [39,45,46]. Niobium oxynitride as a precursor led to niobium carbonitride [47], and complete removal of the nitrogen required high temperatures [9]. By employing metal powders as reducing agents, NbC has been prepared at temperatures as low as 550 °C [48,49].

4.1.2 Formation of mixed molybdenum-niobium carbides from both types of precursor

The effect of combining two metals emerges most clearly for the well-defined precursors. The mixed oxide obtained through calcination of the FD precursor is characterized by the MoO_3(*oP*16) structure, that is, niobium is incorporated while the MoO_3 structure is retained. The origin of the extra reflection could not be clarified. The position at 22.30 °2θ does not align with the reflection of Nb_2O_5(*hP*7) at 22.625 °2θ, and the second large reflection of this oxide at 28.611 °2θ is absent. The substitution of cations of lower valence into a metal oxide, here Nb^{5+} instead of Mo^{6+}, implies oxygen vacancies. The reduction of the mixed oxide was much more facile than that of pure MoO_3, the first step occurred at 140 °C lower temperature, and the second one at 50 °C lower temperature, as evident in TG traces and water formation profiles (Figure 3). This effect can be ascribed to oxygen vacancies, whose presence is known to accelerate oxygen diffusion [50]. In particular, the first step occurs much earlier for the mixed oxide than for pure MoO_3 - at this stage, the pure oxide is presumably free of vacancies. The difference in temperatures becomes less pronounced for the second step, when the suboxides formed during the first reduction with stoichiometries of $MoO_{1.9}$ and Mo_6NbO_{13} (corresponding to $MeO_{1.9}$ with Me=metal) are further reduced.

A similar effect is also seen for the hydrothermally synthesized sample with the lowest niobium content in Figure 1. The traces are more complex because of the initial decomposition of extraneous material relative to the oxides. Independent of this difference, the second reduction step occurs earlier for the mixed metal precursor than for the pure molybdenum precursor.

A general strategy for facilitating the reduction step can be deduced from these observations: metals of lower valence that are incorporated into a precursor may lead to oxygen vacancies, which enhance oxygen mobility and lower the reduction temperature.

A clear trend with composition is seen in the degree of reduction during the first step. Molybdenum-rich samples are further reduced at lower temperatures than niobium-rich samples, which is indicated by the increasing H_2O signal (at about 90 min or 450 °C in Figure 1 and Figure 3) and the lower weight after this step (at about 150 min or 550 °C). With increasing niobium content, methane becomes the more important reductant, and the relative size of the CO signal increases. The profiles also show that the process is drawn out over a temperature range whereas it is a well-defined event for pure molybdenum oxide.

The stoichiometry of the carburization reaction changes with composition; for the transformation of MoO_3 to Mo_2C, 3 oxygen atoms have to be removed and 0.5 carbon atoms have to be introduced per metal atom, whereas for the transformation of Nb_2O_5 to NbC, only 2.5 oxygen atoms have to be removed while 1 carbon atom per metal atom has to be introduced. This exchange of the anion proceeds much more slowly with increasing niobium content, which can be explained by the higher affinity of niobium to oxygen and perhaps also by structures less conducive to oxygen and carbon mobility. The general carbon deficiency of the mixed carbides with NbC structure indicates the difficulty of incorporating carbon, for lack of carbon chemical potential or for poor carbon diffusion. In this context, it is curious that the weight change stops when the CO evolution stops – this correlation suggests that oxygen may be needed and, hence, the earlier loss of oxygen in the form of water, which is promoted by the presence of molybdenum, could be disadvantageous for the carbon incorporation process. Obviously, carburization process parameters including gas composition and total pressure could be optimized, as has been done for tungsten carbides [51,52].

The final carburization temperature of mixed carbides with predominantly Mo_2C(*hP3*) structure was close to that of pure Mo_2C (Figure 3). Formation of CO occurred over a broader

range for the mixed materials; the evolution below 650 °C (which is the temperature of maximum CO evolution for Mo_2C) is ascribed to the beneficial effect of oxygen vacancies or other defects for ion mobility; the evolution at temperatures above 650 °C is ascribed to formation of small amounts of materials with cubic NbC structure (cf. diffractograms 9 and 10 in Figure 5).

All final carburization temperatures of mixed carbides with NbC(*cF*8) structure were between those of the pure carbides, implying that the presence of molybdenum decreases the temperature for formation of this carbide. Several factors affect the carbide formation, immediately relevant are the ability of the surface to activate methane and the mobility of oxygen and carbon in the bulk. In addition, while surface carbon is needed as a driving force, excessive carbon accumulation leads to inertization and must be prevented, which can be achieved through carbon hydrogenation by activated H_2 or through carbon oxidation by residual oxygen emerging from the bulk. From research on methane aromatization, it is well known that MoO_x species are able to activate methane [53] whereas no such reports exist for NbO_x; and NbC is much less active in methane activation than Mo_2C [54]. Consistent with these reports, significant CO evolution in molybdenum-containing precursors occurred at much lower temperature than in niobium-only precursors. If the molybdenum content is low, then carbon accumulation becomes an issue once the oxygen is consumed, as can be seen from the behavior of the sample with x_{Nb} = 0.7, which rapidly gains weight at the end of the carburization. The presence of molybdenum lowers the final carburization temperature; possible reasons are a defective lattice allowing for higher mobility.

A new approach to synthesize niobium carbide at low final carburization temperature, without carbon contamination on the surface, emerges from these observations. The addition of another metal cation such as molybdenum into the niobium precursor apparently suffices to lower the carburization temperature and can be an alternative to addition of nickel or other metallic reductants. However, a significant amount of molybdenum was required.

4.2 Characterization of carbides

4.2.1 Structure and composition

The diffractograms in Figure 5 demonstrate that phase-pure mixed metal carbides could be obtained in the range x_{Nb}= 0.36 to x_{Nb} =1 using hydrothermally synthesized precursors. Phase-pure carbides with a composition in this range could also be obtained via the freeze-drying method,

519 whereas carbides more rich in molybdenum prepared by either synthesis method were not phase
520 pure. Both methods of precursor synthesis are thus principally successful.

521 The hydrothermal method produced precursors that did not contain too much extraneous
522 material and could be carburized successfully without prior calcination. However, the yields were
523 low, implying a significant amount of waste solution. Most importantly, the stoichiometry could
524 not be fully controlled because of the preferential incorporation of niobium in the precursor (Figure
525 4). Loss of molybdenum during carburization as a reason for the enrichment in niobium was
526 excluded on the basis of prior observations [17]. It was not possible to prepare materials with a
527 metal ratio of Mo/Nb larger than 2 that after carburization would form a single phase molybdenum-
528 niobium carbide. The FD method has several advantages over the hydrothermal method, including
529 producing less waste and allowing full control of the stoichiometry. A potential drawback is the
530 additional calcination step that may be advisable to remove excess ions from the starting materials.
531 The advantage of these two synthesis methods over other reported methods is the more intimate
532 mixing of precursor metals, which results in phase-pure materials over a wider range of
533 compositions. Physical mixtures of oxide or nitrates, even if milled or slurried [20,29], do not
534 provide atomic level mixing. Dissolution with subsequent solvent removal, which has also been
535 used for precursor formation [55], can result in sequential precipitation. An advantage of these
536 reported methods is that no starting material is wasted (as with the FD method reported here), and
537 physical mixing completely avoids wet chemistry.

538 The phase-pure materials crystallized in either of two different structures; molybdenum-rich
539 materials formed hexagonal Mo_2C(*hP*3, $P6_3/mmc$) (NiAs type) and niobium-rich materials formed
540 the cubic structure characteristic of both NbC(*cF*8, $Pm\bar{3}m$) (NaCl type) and the isostructural MoC,
541 respectively. The reported lattice constants for the pure carbides are 4.47 Å for NbC (ICDD # 00-
542 038-1364) and 4.281 Å for MoC (ICDD # 03-065-8092), and the trend to higher angles seen in
543 Figure 6 with increasing molybdenum content reflects this shrinkage of the unit cell. The cubic
544 structure seems to be preferred over a wide range, which was also observed by Yu et al. [29] who
545 succeeded in preparing phase-pure materials with x_{Nb} of 0.36 and 0.4. The series of samples with
546 the cubic structure fits well on a Vegard's Law plot (Figure 6), implying true solid solutions. The
547 equilibrium Gibbs free energy will determine whether the structure of the carbide is cubic or
548 hexagonal. Cubic NbC is more stable than hexagonal Mo_2C [56], which explains why over most

549 of the compositional range, it is the preferred structure. Mixtures of phases appeared towards the
550 molybdenum-rich end of the series. This behavior is consistent with calculations that show
551 MoC(*cF*8) to be endergonic and thus less stable than NbC(*cF*8) or Mo_2C(*hP*3) [56], promoting
552 the segregation into two phases. No evidence was found for incorporation of niobium into the
553 Mo_2C structure, which explains why even at low niobium concentrations a second phase appears.

554 The weight losses observed during carburization of the calcined freeze-dried materials are
555 close to the theoretical weight losses and indicate that conversion to carbides is complete. Others
556 have observed formation of oxycarbides [57]; comparison of experimental conditions shows that
557 the process may be sensitive to any of a number of parameters, such as precursor type, heating
558 rate, or final temperature. Except for the pure molybdenum and niobium carbides, the materials
559 were noticeably carbon-deficient, even if a stoichiometry of only one carbon atom per two
560 molybdenum atoms was assumed, also for the NbC/MoC structure (Table 1). Calculations have
561 shown that carbon vacancies increase or do not affect the stability of these cubic carbides [56].

562 *4.2.2 Textural and surface properties*

563 The properties of Mo_2C from a hydrothermally synthesized precursor were similar to those of
564 Mo_2C from commercial MoO_3. The oxygen uptake was less at 2.49 wt% compared to literature
565 values of 3.1 wt%, corresponding to the relative surface areas [17]. The CO uptake at 18.5 µmol/g
566 was slightly higher than the 15.5 µmol/g for a MoO_3-derived carbide but given the generally large
567 variation of such values depending on the method of preparation, this Mo_2C can be considered to
568 be reasonably similar to reported materials. This similarity allows the conclusion that carbides can
569 be obtained from hydrothermally synthesized precursors, and that an intermediate calcination step
570 is not necessary.

571 The surface of NbC obtained from the hydrothermally synthesized precursor was inert. There
572 was no oxygen or CO uptake. It is reported that oxygen dissociatively adsorbs on clean NbC (100)
573 and NbC (111) surfaces [58,59]. Possible explanations for the inertness are a surface that was never
574 fully reduced or a surface covered with a carbon layer. In the literature, NbC generated at a
575 temperature of 900 °C [20] exhibited metallic sites for CO adsorption. The temperature applied
576 here for carburization did not differ much from that in the literature, 950 °C, which should ensure
577 full conversion to NbC [39], as also found by XRD. There was no mass gain observed by TG at
578 the end of the carburization that would suggest carbon uptake, and the elemental analysis suggests

only a small excess over the stoichiometric amount (12 vs. 11.4 wt%). As much as 18 wt% carbon have been reported [39]. Various procedures for surface cleaning can be found in the literature. Some authors [20] have successfully increased the number of CO adsorption sites by treating NbC at 350 °C in O_2 followed by reduction at 450 °C. Others [47] report that surface cleaning to remove deposited carbon can be done at high temperatures (950 °C) with H_2 and not with O_2. It was attempted in this work to oxidize the surface of NbC and then re-carburize the niobium oxycarbide, but a temperature of 950 °C was still needed for complete carburization and removal of oxygen from surface (as indicated by evolution of CO). This behavior demonstrates that oxygen can adsorb very strongly on the surface of niobium. The surface area of NbC was significant at 17 m^2/g although it was synthesized at 950 °C; possibly, the inert surface inhibited sintering.

The properties of the mixed molybdenum-niobium carbides were found to be determined by the actual composition and the final carburization temperature T_f (2^{nd} and 3^{rd} column in Table 1). Even though the temperatures were equal to or higher than that used for Mo_2C, all mixed carbides exhibited higher surface areas and higher pore volumes than Mo_2C. Niobium obviously has a positive effect on surface area, which maybe counteracted to some extent by the need for a higher carburization temperature with increasing niobium content. The highest surface areas exceed those reported for mixed molybdenum-niobium carbides, which reach values of 44 m^2/g [20] and are closer to those reported for molybdenum-niobium oxycarbides [29]. Trends in oxygen uptake reflect trends in surface area but there is no strict proportionality. There are two possible explanations: surface areas were measured after passivation, which is known to alter (*i.e.*, reduce) surface area; and the surface may become more inert towards O_2 with increasing niobium content, approaching the properties of pure NbC. The maximum surface area and oxygen uptake occurred around $x_{Nb} = 0.5$.

The number of sites titrated by CO chemisorption steadily increased with increasing molybdenum content (Table 1), which for many samples opposes the trend seen in oxygen chemisorption during passivation. This behavior can be explained by the differences between the sites on which oxygen and CO chemisorb. Oxygen chemisorbs on all metallic sites whereas CO chemisorbs selectively on noble metal-like sites [18]. The observed relationship of CO uptake with composition also suggests that the surfaces of these mixed carbides, unlike those of previously

608 described tungsten-molybdenum [19] and molybdenum-niobium carbides [21], were not enriched
609 in molybdenum.

610 **4.3 Reduction after passivation**

611 The TPR data (Figure 7) show that depending on the temperature, oxygen or carbon can be
612 removed from molybdenum-containing carbides, whereas neither oxygen nor carbon could be
613 removed from NbC by H_2 treatment at temperatures up to 700 °C. Mo_2C obtained from a
614 hydrothermally synthesized precursor behaved like MoO_3-derived Mo_2C [17]. Reduction of the
615 passivated surface in H_2 was fastest at a temperature slightly above 150 °C. Methane release, which
616 required a temperature of 600 °C, was insignificant, suggesting no carbon removal from the bulk.

617 Surface reduction, analogous to bulk reduction, was promoted on the mixed metal carbides, as
618 indicated by the pronounced shoulder in the water evolution profile at 100 °C. Sites with a lower
619 oxygen binding energy could result from electronic effects that weaken chemisorption of oxygen
620 on the surface or from highly oxidized metal atoms associated with edge and corner sites (for high
621 surface area and correspondingly small particle size). In molybdenum-niobium carbide, electron
622 density is removed from both molybdenum and the molybdenum-carbon covalent bond relative to
623 the situation in molybdenum carbide [60]. This charge relocation could also explain a weaker
624 binding of other anionic species.

625 For samples with x_{Nb}=0.38 or 0.51 prepared via hydrothermal synthesis, ethane evolved at 300
626 °C. The C_xH_y fragments may have been formed during carburization, and are hydrogenated and
627 volatilized during TPR.

628 Methane formation was promoted and substantial for materials of intermediate composition
629 (traces 3, 4, 5 in Figure 7) indicating facile creation of carbon vacancies on the surface and in the
630 bulk. The relocation of electron density described above could be the reason for weaker metal-
631 carbon bonds and facile carbon vacancy formation. This property distinguishes the mixed carbides
632 from Mo_2C and NbC. The creation of vacancies as active sites is important for reactions such as
633 direct desulfurization [61], and may be the reason that molybdenum-niobium carbides are active
634 for hydrotreating [21,29].

4.4 Catalytic performance

At a reaction temperature of 250 °C and 21 bar pressure, methylcyclohexane was the only product, that is, the ability of the catalyst to activate H_2 and adsorb toluene such that ring hydrogenation can occur was probed. NbC did not show any activity, consistent with its generally inert behavior. Addition of molybdenum resulted in an increasing number of noble metal-like sites according to the CO uptake values in Table 1. Principally in agreement with this trend, the hydrogenation activity (relative to catalyst mass) increased, which is conceivable since it is associated with the metallic behavior of metal carbides. However, TOFs (Figure 8, referenced to CO uptake) increased significantly with increasing molybdenum content, implying a change in the quality of the sites. The different bulk structures could play a role; the mixed carbides with the cubic structure of NbC/MoC were characterized by similar TOF_S for hydrogenation, whereas carbides with the hexagonal structure of Mo_2C enabled higher TOFs. Molybdenum carbide itself can be prepared in various structures including hexagonal Mo_2C(*hP*3), cubic Mo_2C(*cF*6), and cubic MoC(*cF*8). A complete understanding of the catalytic behavior associated with these phases is lacking. Mo_2C(*cF*6) is reported to have a higher specific activity than Mo_2C(*hP*3) for hydrogenation of CO whereas Mo_2C(*hP*3) was found to be 200 times more active for hydrogenolysis of ethane than Mo_2C(*cF*6), which was ascribed to differences in the structure of the main exposed planes [62]. For hydrogenation of toluene, Mo_2C(*cF*6) was characterized by a one order of magnitude higher rate per area than (commercially acquired) hexagonal-phase molybdenum carbide [63], but the calculation was based on the assumption that the surface area of Mo_2C(*cF*6) scaled with its mass fraction of 11% in the sample (which also contained MoO_2 and C). CO uptakes were available in some cases [62], and differed by much less than the reaction rates, suggesting that for certain reactions, TOFs can indeed vary significantly for different structures.

At 400 °C, as at 250 °C, carbides rich in molybdenum with hexagonal Mo_2C structure were more active than those rich in niobium. While the samples with high molybdenum content deactivated more rapidly, the total amount of toluene converted in 24 hours on stream was much higher for these samples than for the less active niobium-rich samples. Products indicative of multifunctional catalysis were observed at 400 °C (Table 2). Ring hydrogenation and hydrogenolysis to short alkanes reflect the metallic function, whereas ring contraction to

665 cyclopentanes and disproportionation to benzene and xylenes indicate acid sites. Dealkylation to
666 benzene can be catalyzed by a variety of sites, including acid and metallic sites.

667 The molybdenum carbide Mo_2C(*hP*3) is known to have pronounced metallic behavior that
668 favors hydrogenation and hydrogenolysis. At a niobium content of x_{Nb} = 0.14, the structure is still
669 predominantly Mo_2C(*hP*3) and the metallic behavior is conserved with ring hydrogenation to
670 methylcyclohexane and hydrogenolysis to small alkanes being the predominant reactions.
671 Calculations show that substitution of molybdenum by niobium does not alter the electronic
672 structure of Mo_2C significantly, whereas substitution of carbon by oxygen increases ionicity [60].
673 Here, a higher fraction of niobium and a change in structure have three effects: the activity is lower
674 (as indicated by the W/F that was needed to adjust to equal conversion, Table 2), hydrogenolysis
675 is suppressed, and ring contraction is promoted. The residual amount of oxygen (remaining after
676 passivation and reduction, Table 1) seems to be too small to explain the dramatic decrease in
677 toluene TOF with incorporation of niobium (Figure 8). More likely are geometric effects resulting
678 from a much higher surface area and correspondingly smaller particle size, which are equivalent
679 to a loss of ensemble sites. At least on noble metals, toluene hydrogenation is structure-sensitive
680 [64,65] as is alkane hydrogenolysis [66].

681 The ring contraction products can be ascribed to Brønsted acid sites that are associated with
682 the residual oxygen on the surface of these materials (Table 1, x_{Nb}=0.38 or 0.51). Niobium
683 oxycarbides have mainly been tested for HDS [29], and little is known about a catalytic
684 contribution of acid sites. In contrast, tungsten and molybdenum surface oxycarbides can provide
685 acid sites, which, for example, catalyze alkane isomerization [11,14]. The majority of sites on
686 partially oxidized mixed molybdenum-tungsten carbides are Brønsted acid sites [67]. The source
687 of the oxygen affinity here is evidently the niobium, in line with prior reports. In the case of mixed
688 molybdenum-niobium carbides, oxygen tends to adsorb preferentially on niobium [29]. Also,
689 niobium nitride can adsorb more oxygen than molybdenum or tungsten nitride, because of the
690 higher affinity of niobium to oxygen [68]. Niobium forms oxides with stoichiometries NbO,
691 Nb_2O_3, NbO_2 and Nb_2O_5 with different catalytic properties [69]. The pentoxide, Nb_2O_5, possesses
692 strong Brønsted acid sites with H_o between -5.6 and -8.2 as well as Lewis acid sites [70]. Niobium
693 (III) oxide would be expected to have less acidic OH groups than the (V) oxide, according to trends
694 in the periodic table. On the surface of the mixed carbide, species reminiscent of the surface

structure of these oxides may be present and provide acid sites. It is established in the literature [71,72] that ring contraction needs strong acid sites such as those in zeolites or on sulfated zirconia. Further differentiation can be made; ethylcyclopentane can be formed on a range of strong acid sites, whereas significant formation of dimethylcyclopentane requires very strong acid sites as can be found in the structures FAU, MOR, or BEA [72]. The formation of ring contraction products indicates that strongly acidic Brønsted sites are present on the mixed molybdenum-niobium carbides although the sites are not sufficient in strength to produce predominantly dimethylcylcopentanes.

The formation of disproportionation products at 400 °C, benzene and xylene, is an indication of acid sites. Toluene disproportionation is typically conducted using MFI zeolites as catalysts, and the activity scales with the strength of the Brønsted acid sites [73].

The benzene excess over xylenes can be explained by dealkylation on acid sites or hydrodealkylation on metallic sites [74]. The selectivity, as represented by the benzene excess, varies between 4.9 and 6.9% and is highest when the disproportionation selectivity is highest, suggesting this pathway may be catalyzed by acid sites. Dealkylation has been claimed to be promoted by the presence of both Brønsted and Lewis acid sites [**Error! Bookmark not defined.**], or to require stronger acid sites than disproportionation [75]. However, overall the benzene excess is only weakly dependent on catalyst composition and hydrodealkylation as a pathway cannot be ruled out.

In summary, the catalytic behavior of the mixed carbides depends on the balance between metallic and acidic sites. In the hydrogenation of toluene on platinum, addition of the 5^{th} hydrogen has been identified as the rate-determining step [76]. Assuming a similar scenario on carbides, desorption of methylcyclohexene and, depending on the number of metallic sites versus number of acid sites, hydrogenation and hydrogenolysis or ring contraction can occur. The data in Table 2 suggest that there may be in optimum niobium content with respect to ring contraction selectivity, but a broader data base would be needed to confirm this observation. The trend from more metallic to more acidic behavior with increasing niobium content is consistent with the behavior of the corresponding nitrides. Molybdenum oxynitride has been compared with niobium oxynitride for metal-catalyzed reactions (hydrogenation of toluene) and acid-catalyzed reactions (isomerization

of cyclohexane) and results revealed that molybdenum oxynitride has more pronounced metallic behavior whereas niobium oxynitride has more pronounced acid behavior [77].

5 Conclusions

Single-phase mixed metal carbides of molybdenum and niobium with various compositions were prepared by carburizing precursors with atomic level mixing of metal ions. Both hydrothermal synthesis and flash-freezing with subsequent freeze-drying were suitable to obtain such precursors. The presence of two metals caused reduction and carburization to occur at lower temperatures compared to the synthesis of the pure metal carbides. Based on the metal ratios and method of precursor synthesis, the cubic NbC/MoC structure or the hexagonal Mo_2C structure was preferably formed. Single-phase mixed metal carbides with the cubic NbC/MoC structure were obtained at niobium mole fractions between 0.38 and 1. Mixed metal carbides with a niobium mole fraction less than 0.38 were a mixture of the cubic NbC/MoC structure and the hexagonal Mo_2C structure. Samples prepared from hydrothermally precipitated precursors were characterized by surface areas exceeding 50 m^2/g and high oxygen uptakes during passivation. TPR data showed that creation of carbon vacancies or surface reduction is more facile for mixed metal carbides compared to their monometallic counterparts. The number of metallic sites as probed by CO chemisorption increased with increasing molybdenum content. Carbides with high molybdenum fraction and hexagonal Mo_2C structure yielded more metal-catalyzed products (hydrogenation and hydrogenolysis) during toluene conversion, whereas carbides with high niobium fraction and cubic NbC/MoC structure were less active and produced more acid-catalyzed products. At a niobium metal fraction of x_{Nb}=0.14, the ring hydrogenation TOF (based on CO adsorption sites) was decreased by a factor of six relative to Mo_2C. At equal conversion, the selectivity for ring opening products was 32% for a mixed metal carbide with x_{Nb}=0.38 vs. 0% for Mo_2C. These results demonstrate that the bulk and surface properties of carbides can be tuned by tuning the composition and that the strategy to improve oxygen retention on carbide surfaces by incorporating a more oxophilic metal is successful.

Acknowledgements

Acknowledgment is made to the Donors of the American Chemical Society Petroleum Research Fund for support (or partial support) of this research under PRF#51448-ND5. This work

754 was, in part, supported by NSF award 0923247 (thermal analysis equipment as part of a major
755 research instrumentation grant). The authors thank Lance L. Lobban for providing the test reactor
756 and Alana Denning for her assistance with EDX measurements.

757 **References**

[1] J.H. Sinfelt, D.J.C. Yates, Effect of carbiding on hydrogenolysis activity of molybdenum, Nature Phys. Sci. 229 (1971) 27.

[2] R.B. Levy, M. Boudart, Platinum-like behavior of tungsten carbide in surface catalysis, Science, New Series 181 (1973) 547-549.

[3] S.T. Oyama, Preparation and catalytic properties of transition metal carbides and nitrides, Catal. Today 15 (1992) 179-200.

[4] S.T. Oyama, Transition metal carbides, nitrides, and phosphides, in Handbook of Heterogeneous Catalysis, Vol. I, Eds. G. Ertl, H. Knözinger, F. Schüth, J. Weitkamp, 2nd edition, Wiley-VCh, 2008, pp. 342-356.

[5] E. Furimsky, Metal carbides and nitrides as potential catalysts for hydroprocessing, Appl. Catal. A: General 240 (2003) 1–28.

[6] K. Xiong, W. Yu, J.G. Chen, Selective deoxygenation of aldehydes and alcohols on molybdenum carbide (Mo_2C) surfaces, Appl. Surf. Sci. 323 (2014) 88–95.

[7] W.-S. Lee, Z. Wang, R.J. Wu, A. Bhan, Selective vapor-phase hydrodeoxygenation of anisole to benzene on molybdenum carbide catalysts, J. Catal. 319 (2014) 44-53.

[8] D.J. Ham, J.S. Lee, Transition metal carbides and nitrides as electrode materials for low temperature fuel cells, Energies 2 (2009) 873-899.

[9] C. Chagas, R. Pfeifer, A. Rocha, V. Teixeira da Silva, Synthesis of niobium carbonitride by thermal decomposition of guanidine oxaloniobate and its application to the hydrodesulfurization of dibenzothiophene, Topics Catal. 55 (2012) 910-921.

[10] F.H. Ribeiro, M. Boudart, R.A. Dalla Betta, E. Iglesia, Catalytic reactions of *n*-alkanes on β-W_2C and WC: The effect of surface oxygen on reaction pathways, J. Catal. 130 (1991) 498-513.

[11] E. Iglesia, J.E. Baumgartner, F.H. Ribeiro, M. Boudart, Bifunctional reactions of alkanes on tungsten carbides modified by chemisorbed oxygen, J. Catal. 131 (1991) 523-544.

[12] E. Iglesia, F.H. Ribeiro, M. Boudart, J.E. Baumgartner, Synthesis, characterization, and catalytic properties of clean and oxygen-modified tungsten carbides, Catal. Today 15 (1992) 307-337.

[13] P. Delporte, F. Meunier, C. Pham-Huu, P. Vennegues, M.J. Ledoux, J. Guille, Physical characterization of molybdenum oxycarbide catalyst; TEM, XRD and XPS, Catal. Today 23 (1995) 251-267.

[14] P. Delporte, C. Pham-Huu, M.J. Ledoux, Effect of the reaction temperature and hydrocarbon partial pressure on the activity of carbon-modified MoO_3 for *n*-hexane isomerization, Appl. Catal. A: General 149 (1997) l51–180.

[15] C. Bouchy, C. Pham-Huu, B. Heinrich, E.G. Derouane, S.B. Derouane-Abd Hamid, M.J. Ledoux, In situ TPO, TPD and XRD characterisation of a molybdenum oxycarbohydride catalyst for *n*-butane isomerization, Appl. Catal. A: General 215 (2001) 175–184.

[16] A.J. Medford, A. Vojvodic, F. Studt, F. Abild-Pedersen, J.K. Nørskov, Elementary steps of syngas reactions on Mo_2C(001): Adsorption thermochemistry and bond dissociation, J. Catal. 290 (2012) 108-117.

[17] A. Mehdad, R.E. Jentoft, F.C. Jentoft, Passivation agents and conditions for Mo_2C and W_2C: Effect on catalytic activity for toluene hydrogenation, J. Catal. 347 (2017) 89-101.

[18] J.-S. Choi, G. Bugli, G. Djéga-Mariadassou, Influence of the degree of carburization on the density of sites and hydrogenating activity of molybdenum carbides, J. Catal. 193 (2000) 238-247.

[19] L. Leclercq, M. Provost, H. Pastor, G. Leclercq, Catalytic properties of transition metal carbides II. Activity of bulk mixed carbides of molybdenum and tungsten in hydrocarbon conversion, J. Catal. 117 (1989) 384-395.

[20] V.L.S. Teixeira da Silva, M. Schmal, V. Schwartz, S.T. Oyama, Synthesis of a Mo/Nb mixed carbide, J. Mater. Res. 13 (1998) 1977-1988.

[21] V. Schwartz, S.T. Oyama, J.G. Chen, Supported bimetallic Nb−Mo carbide: Synthesis, characterization, and reactivity, J. Phys. Chem. B 104 (2000) 8800-8806.

[22] T.-C. Xiao, A.P.E. York, H. Al-Megren, J.B. Claridge, H.-T. Wang, M.L.H. Green, Preparation of molybdenum carbide-based catalysts for deep HDN, C. R. Acad. Sci. Paris, Série IIc, Chimie: Chemistry 3 (2000) 451–458.

[23] T.-C. Xiao, A.P. E. York, H. Al-Megren, C.V. Williams, H.-T. Wang, M.L.H. Green, Preparation and characterisation of bimetallic cobalt and molybdenum carbides, J. Catal. 202 (2001) 100–109.

[24] T. Xiao, H. Wang, A.P. E. York, V.C. Williams, M.L.H. Green, Preparation of nickel–tungsten bimetallic carbide catalysts, J. Catal. 209 (2002) 318–330.

[25] T.-C. Xiao, A. Hanif, A.P.E. York, M.L.H. Green, Methane partial oxidation to synthesis gas over bimetallic cobalt/tungsten carbide catalysts and integration with a Mn substituted hexaaluminate combustion catalyst, Catal. Today 147 (2009) 196–202.

[26] H.A. Al-Megren , S.L. González-Cortés, T. Xiao, M.L.H. Green, A comparative study of the catalytic performance of Co-Mo and Co(Ni)-W carbide catalysts in the hydrodenitrogenation (HDN) reaction of pyridine, Appl. Catal. A: General 329 (2007) 36–45.

[27] D.J. Haynes, D.A. Berry, D. Shekhawat, T.-C. Xiao, M.L.H. Green, J.J. Spivey, Partial oxidation of *n*-tetradecane over 1 wt % Pt/γ-Al_2O_3 and $Co_{0.4}Mo_{0.6}C_x$ carbide catalysts: A comparative study, Ind. Eng. Chem. Res. 47 (2008) 7663–7671.

[28] B. Frank, T.P. Cotter, M.E. Schuster, R. Schlögl, A. Trunschke, Carbon dynamics on the molybdenum carbide surface during catalytic propane dehydrogenation, Chem. Europ. J. 19 (2013) 16938-16945.

[29] C.C. Yu, S. Ramanathan, B. Dhandapani, J.G. Chen, S.T. Oyama, Bimetallic Nb−Mo carbide hydroprocessing catalysts: Synthesis, characterization, and activity studies, J. Phys. Chem. B 101 (1997) 512-518.

[30] C. Marquez-Alvarez, J.B. Claridge, A.P.E. York, J. Sloan, M.LH. Green, Benzene hydrogenation over transition metal carbides, Stud. Surf. Sci. Catal. 106 (1997) 485–490.

[31] L.C. A. Bastos, W.R. Monteiro, M.A. Zacharias, G.M. da Cruz, J. Augusto, J. Rodrigues, Preparation and characterization of Mo/W bimetallic carbides by using different synthesis methods, Catal. Lett. 120 (2008) 48–55.

[32] L. Leclercq, M. Provost, H. Pastor, J. Grimblot, A.M. Hardy, L. Gengembre, G. Leclercq, Catalytic Properties of Transition Metal Carbides I. Preparation and physical characterization of bulk mixed carbides of molybdenum and tungsten, J. Catal. 117 (1989) 371-383.

[33] T.-H. Nguyen, A.A. Adesina, E.M.T Yue, Y.-J. Lee, A. Khodakov, M.P. Brungs, Synthesis of Mo–W carbide via propane carburization of the precursor sulfide: Kinetic analysis, J. Chem. Technol. Biotechnol. 79 (2004) 286–290.

[34] S. Ramanathan, S.T. Oyama, New catalysts for hydroprocessing: Transition metal carbides and nitrides, J. Phys. Chem. 99 (1995) 16365-16372.

[35] M.K. Neylon, S. Choi, H. Kwon, K.E. Curry, L.T. Thompson, Catalytic properties of early transition metal nitrides and carbides: *n*-butane hydrogenolysis, dehydrogenation and isomerization, Appl. Catal. A: General 183 (1999) 253-263.

[36] T. Murayama, N. Kuramata, S. Takatama, K. Nakatani, S. Izumi, X. Yi, W. Ueda, Synthesis of porous and acidic complex metal oxide catalyst based on group 5 and 6 elements, Catal. Today 185 (2012) 224-229.

[37] A. El-Himri, F. Sapiña, R. Ibáñez, A. Beltrán, Synthesis of new vanadium-chromium and chromium-molybdenum oxynitrides by direct ammonolysis of freeze-dried precursors, J. Mater. Chem. 10 (2000) 2537-2541.

[38] A. El-Himri, P. Núñez, F. Sapiña, R. Ibáñez, A. Beltrán, J.-M. Martínez-Agudoc, Synthesis of new molybdenum–tungsten, vanadium–tungsten and vanadium–molybdenum–tungsten oxynitrides from freeze-dried precursors, J. Solid State Chem. 177 (2004) 2423–2431.

[39] V.L.S. Teixeira da Silva, M. Schmal, S.T. Oyama, Niobium carbide synthesis from niobium oxide: study of the synthesis conditions, kinetics, and solid-state transformation mechanism, J. Solid State Chem. 123 (1996) 168-182.

[40] J.S. Lee, S.T. Oyama, M. Boudart, Molybdenum carbide catalysts I. Synthesis of unsupported powders, J. Catal. 106 (1987) 125-133.

[41] D.E. Wobbe, W.A. Noyes, Photochemical studies IV The thermal decomposition of anhydrous oxalic acid and its relation to the photochemical decomposition, J. Am. Chem. Soc. 48 (1926) 2856-2868.

[42] Y. Okada, E. Sasaki, E. Watanabe, S. Hyodo, H. Nishijima, Development of dehydrogenation catalyst for hydrogen generation in organic chemical hydride method, Int. J. Hydrogen Energy 31 (2006) 1348–1356.

[43] A. Hanif, T. Xiao, A.P.E. York, J. Sloan, M.L.H. Green, Study on the structure and formation mechanism of molybdenum carbides, Chem. Mater. 14 (2002) 1009-1015.

[44] F.A.O. Fontes, J.F. de Sousa, C.P. Souza, M.B.D. Bezerra, M. Benachour, Production of NbC from Nb_2O_5 in a rotating cylinder reactor: Kinetic study of reduction/carburization reactions, Chem. Engr. J. 175 (2011) 534-538.

[45] V.L.S. Teixeira da Silva, E.I. Ko, M. Schmal, S.T. Oyama, Synthesis of niobium carbide from niobium oxide aerogels, Chem. Mater. 7 (1995) 179-184.

[46] S. Witkowski, M. Ruszak, C. Sayag, J. Pielaszek, G. Djéga-Mariadassou, Nanocrystalline NbC formation from mesostructured niobium oxide studied by HRTEM, SAED and in situ XRD, Appl. Catal. A: General 307 (2006) 205-211.

[47] H.S. Kim, G. Bugli, G. Djéga-Mariadassou, Preparation and characterization of niobium carbide and carbonitride, J. Solid State Chem. 142 (1999) 100-107.

[48] L. Shi, Y. Gu, L. Chen, Z. Yang, J. Ma, Y. Qian, Synthesis and oxidation behavior of nanocrystalline niobium carbide, Solid State Ionics, 176 (2005) 841-843.

[49] J. Ma, M. Wu, Y. Du, S. Chen, W. Jin, L. Fu, Q. Yang, A. Wen, Formation of nanocrystalline niobium carbide (NbC) with a convenient route at low temperature, J. Alloys Comps. 475 (2009) 415-417.

[50] M. Martin, Diffusion in oxides, in Diffusion in Condensed Matter: Methods, Materials, Models, Editors: Heitjans, Paul, Kärger, Jörg (Eds.), 2005 Springer-Verlag Berlin Heidelberg, p. 209-247.

[51] G. Leclercq, M. Kamal, J. M. Giraudon, P. Devassine, L. Feigenbaum, L. Leclercq, A. Frennet, J. M. Bastin, A. Löfberg, S. Decker, M. Dufour, Study of the preparation of bulk powder tungsten carbides by temperature programmed reaction with $CH_4 + H_2$ mixtures, J. Catal. 158 (1996) 142–169.

[52] A. Löfberg, A. Frennet, G. Leclercq, L. Leclercq, J.M. Giraudon, Mechanism of WO_3 reduction and carburization in CH_4/H_2 mixtures leading to bulk tungsten carbide powder catalysts, J. Catal. 189 (2000) 170–183.

[53] J. Gao, Y. Zheng, J.-M. Jehng, Y. Tang, I.E. Wachs, S.G. Podkolzin, Identification of molybdenum oxide nanostructures on zeolites for natural gas conversion, Science 348 (2015) 686-690.

[54] A.C. Camacho Rodrigues, J.L. Fontes Monteiro, Effect of the introduction of niobium carbide on non-oxidative dehydro-aromatization of methane over MoMCM-22, Reac. Kinet. Mech. Cat. 105 (2012) 441–450.

[55] X.-H. Wang, M.-H. Zhang, W. Lia, K.-Y. Tao, A simple synthesis route and characterisation of Co_3Mo_3C, Dalton Trans. (2007) 5165–5170.

[56] H.W. Hugosson, O. Eriksson, U. Jansson, B. Johansson, Phase stabilities and homogeneity ranges in 4d-transition-metal carbides: A theoretical study, Phys. Rev. B 63 (2001) 134108.

[57] S. Ted Oyama,1 C. Charles Yu, S. Ramanathan, Transition metal bimetallic oxycarbides: synthesis, characterization, and activity studies, J. Catal. 184 (1999) 535–549.

[58] K. Edamoto, T. Anazawa, E. Shiobara, M. Hatta, E. Miyazaki, H. Kato, S. Otani, Oxygen adsorption on a $NbC_{0.9}$ (111) surface: Angle-resolved photoemission study, Phys. Rev. B 43 (1991) 3871-3875.

[59] T. Aizawa, W. Hayami, R. Souda, S. Otani, T. Tanaka, Y. Ishizawa, Molecular adsorption of oxygen on transition-metal carbide, Surf. Sci. 357–358 (1996) 645-650.

[60] H.W. Hugosson, L. Nordström, U. Jansson, B. Johansson, O. Eriksson, Theoretical studies of substitutional impurities in molybdenum carbide, Phys. Rev. B 60 (1999) 15123-15130.

[61] M. Egorova, R. Prins, Hydrodesulfurization of dibenzothiophene and 4,6-dimethyldibenzothiophene over sulfided NiMo/γ-Al_2O_3, CoMo/γ-Al_2O_3, and Mo/γ-Al_2O_3 catalysts, J. Catal. 225 (2004) 417-427.

[62] G.S. Ranhotra, A.T. Bell, J.A. Reimer, Catalysis over molybdenum carbides and nitrides: II. Studies of CO hydrogenation and C_2H_6 hydrogenolysis, J. Catal. 108 (1987) 40-49.

[63] M.-L. Frauwallner, F. López-Linares, J. Lara-Romero, C.E. Scott, V. Ali, E. Hernández, P. Pereira-Almao, Toluene hydrogenation at low temperature using a molybdenum carbide catalyst, Appl. Catal. A: General 394 (2011) 62-70.

[64] V.V. Pushkarev, K. An, S. Alayoglu, S.K. Beaumont, G.A. Somorjai, Hydrogenation of benzene and toluene over size controlled Pt/SBA-15 catalysts: Elucidation of the Pt particle size effect on reaction kinetics, J. Catal. 292 (2012) 64–72.

[65] P.S.F. Mendes, G. Lapisardi, C. Bouchy, M. Rivallan, J.M. Silva, M.F. Ribeiro, Hydrogenating activity of Pt/zeolite catalysts focusing acid support and metal dispersion influence, Appl. Catal. A: General 504 (2015) 17-28.

[66] D. Nazimek, J. Ryczkowski, Influence of the crystallite size of platinum on the course of hydrogenolysis and isomerization of *n*-butane over Pt/Al_2O_3 catalysts, React. Kinet. Catal. Lett. 40 (1989) 137-143.

[67] A.-F. Lamic, C.-H. Shin, G. Djéga-Mariadassou, C. Potvin, Characterization of new bimetallic oxycarbide ($MoWC_{0.5}O_{0.6}$) for bifunctional isomerization of *n*-heptane, Catal. Lett. 107 (2006) 89-94.

[68] R. Brayner, J.A.J. Rodrigues, G.M. Cruz, Synthesis and molding of niobium oxynitrides with macropores generation: Reactivity and stability in cyclohexane dehydrogenation, Catal. Today 57 (2000) 219-223.

[69] S. Isobe, K. Kudoh, S. Hino, K. Hara, N. Hashimoto, S. Ohnuki, Catalytic efficiency of Nb and Nb oxides for hydrogen dissociation, Appl. Phys. Lett. 107 (2015) 081602.

[70] I. Nowak , M. Ziolek, Niobium compounds: Preparation, characterization, and application in heterogeneous catalysis, Chem. Rev. 99 (1999) 3603-3624.

[71] K. Shimizu, T. Sunagawa, C.R. Vera, K. Ukegawa, Catalytic activity for synthesis of isomerized products from benzene over platinum-supported sulfated zirconia, Appl. Catal. A: General 206 (2001) 79-86.

[72] G.B. McVicker, O.C. Feeley, J.J. Ziemiak, D.E.W. Vaughan, K.C. Strohmaier, W.R. Kliewer, D.P. Leta, Methylcyclohexane ring-contraction: A sensitive solid acidity and shape selectivity probe reaction, J. Phys. Chem. B 109 (2005) 2222-2226.

[74] D.C. Grenoble, The chemistry and catalysis of the toluene hydrodealkylation reaction: I. The specific activities and selectivities of Group VIIB and Group VIII metals supported on alumina, J. Catal. 56 (1979) 32-39.

[75] M.A. Uguina, J.L. Sotelo, D.P. Serrano, J.L. Valverde, Deactivation kinetics of para-selective toluene disproportionation over modified ZSM-5, Ind. Eng. Chem. Res. 33 (1994) 26-31.

[76] M. Saeys, M.-F. Reyniers J.W. Thybaut, M. Neurock, G.B. Marin, First-principles based kinetic model for the hydrogenation of toluene, J. Catal. 236 (2005) 129–138.

[77] H.S. Kim, C. Sayag, G. Bugli, G. Djega-Mariadassou, M. Boudart, Preparation, characterization and catalytic activity of niobium oxynitride and oxycarbide in hydrotreatment, MRS Online Proceedings Library 368 (1994) 3-14.